American Mineralogist, Volume 80, pages 201–212, 1995

In-situ spectroscopic investigation of high-pressure hydrated $(Mg,Fe)SiO_3$ glasses: OH vibrations as a probe of glass structure

C. Closmann, Q. Williams

Earth Science Department and Institute of Tectonics, University of California, Santa Cruz, California 95064, U.S.A.

Abstract

We have investigated the structure of hydrated $(Mg,Fe)SiO_3$ glasses both at high pressure and after quenching, using infrared spectroscopy. Glasses were synthesized by fusion at pressures of up to 41 GPa and probed in situ to 39 GPa. Strong H bonding, as manifested by the presence of distinct OH stretching bands between 2250 and 2600 cm^{-1}, plays an important role in the speciation of OH groups at pressures between 15 and 25 GPa. At higher pressures, strong H bonding is also observed in the glasses but is completely unquenchable to ambient pressure; major structural changes are observed during decompression from pressures in excess of 20 GPa. Both the absence of a significant concentration of strongly H-bound OH groups and the similarity in frequency of the primary O-H stretching peak in the spectra of samples quenched from pressures above 30 GPa and those formed below 15 GPa indicate that similar structural features exist in glasses synthesized and quenched from these two separate pressure regimes. We infer that changes in Si coordination occur primarily between these two pressures and are largely unquenchable. Intratetrahedral H bonding is suggested as a possible mechanism for densification at pressures lower than ~25 GPa. Estimated bond lengths for high-pressure hydroxylated species imply that the hydrous component in silicate melts undergoes significant densification with pressure, and that the volume of dissolved H_2O in high-pressure silicate melts is controlled almost solely by the volume of O anions.

Introduction

The structural state of pressure-densified glasses and melts is important in providing a physical basis for understanding melt rheology, petrogenesis, and melt-solid density contrasts in the deep Earth. Recent work has shown that under deep Earth conditions, basic melts may be denser than coexisting solids (Rigden et al., 1984; Miller et al., 1991; Agee and Walker, 1988, 1993). Such density crossovers have profound implications for the Earth's differentiation history (Agee and Walker, 1993) and may play an important role in maintaining partial melts at depth in the Earth today. For example, Revenaugh and Sipkin (1994) found seismological indications of a thin layer (<40 km) of partial melt above the 410-km discontinuity. In addition, Poisson's ratio in the lower mantle is higher (0.30) than that in any other part of the silicate Earth (Dziewonski and Anderson, 1981), suggesting that the lower mantle could also contain small quantities of partial melt. That such partial melts may exist in the mantle indicates that the structure of such a melt could directly affect deep Earth processes.

Moreover, such melts are likely to be hydrous. Tyburczy et al. (1991) showed that a H_2O content of up to 2 wt% could be consistent with seismological data for the lower mantle, and Revenaugh and Sipkin's (1994) proposed partial melt in the transition zone is probably volatile-rich. Hence, H_2O is a plausible component of melts in the deep Earth. Therefore, detailed investigation of the microscopic mechanisms of hydrous melt and glass densification under compression is crucial for a thorough understanding of the physical changes taking place in mantle melts. To date, there have been almost no data on the structure of hydrous glasses formed under lower mantle conditions (Williams, 1990).

Both experimental and theoretical methods have been used to examine densification processes in silicate liquids and glasses. With increasing pressure, densification mechanisms for silicate glasses include closure of the Si-O-Si angle, distortion and compaction of Si tetrahedra (Hemley et al., 1986; Williams et al., 1993), and ultimately changes in the coordination number of Si. Indeed, studies of diopside, anorthite, silica, and sodium silicate glasses have found that at pressures of 20–30 GPa, densification is dominated by an increase in the coordination of Si by O from fourfold toward sixfold, a transition mediated by tetrahedral distortions (Williams and Jeanloz, 1988; Wolf et al., 1990; Meade et al., 1992; Kubicki et al., 1992; Williams et al., 1993).

The bonding environment and speciation of dissolved H_2O in glasses provides a useful probe of local structural features (McMillan and Remmele, 1986; Susman et al.,

0003–004X/95/0304–0201$02.00

1990; Williams, 1990), and lends insight into how H_2O alters the macroscopic properties of glasses and melts (Hetherington and Jack, 1962; Shelby and McVay, 1976; Watson, 1981; Acocella et al., 1984; White and Montana, 1990). A number of studies at relatively low pressures have shown that for total H_2O contents of up to ~4–6 wt%, H_2O dissolves in melts predominantly as OH groups (Bartholomew et al., 1980; Wu, 1980; Stolper, 1982a; Eckert et al., 1988). The mechanism by which H_2O alters the structure of silicate glasses at these low total H_2O contents is generally agreed to be by reaction of OH groups with a bridging O atom to form SiOH groups, thereby depolymerizing the silicate network (Scholze, 1966; Stolper, 1982a, 1982b; Tomozawa, 1985; White and Montana, 1990; Kümmerlen et al., 1992). Again, however, the effect of very high pressures on H_2O speciation and structural environment remains ill-constrained both at high pressures and after quenching. Indeed, there is significant uncertainty as to which structural features of high-pressure glasses and liquids are quenched to ambient pressures (McMillan and Piriou, 1983; Williams, 1990; Wolf et al., 1990).

Thus, our goals are to examine the overall changes in the structure of hydrous glasses induced by pressure, the changes in the speciation of H_2O as a function of pressure, and the degree to which structural features are preserved on decompression in these glasses. In particular, we obtained infrared spectra of hydrated (Mg,Fe)SiO_3 glasses synthesized at pressure between 5 and 41 GPa, both in situ at high pressures (quenched only in temperature) and upon quench from pressure. As the behavior of OH units (and their vibrations) is well understood at ambient conditions in a wide range of bonding environments (Nakamoto et al., 1955; Novak, 1974), the OH unit represents an ideal probe for structural environments in high-pressure amorphous samples. We infer that pressure-induced changes in the OH stretching region of the spectrum are sensitive to the coordination environment of Si and that glasses quenched from a pressure regime in which $^{[6]}$Si dominates the glass structure closely resemble glasses quenched from the lowest pressures of our study. Additionally, we present evidence for intratetrahedral H bonding as a densification mechanism for glasses in the $^{[4]}$Si regime. Thus, our experiments illuminate the structural behavior of hydrous glasses and, by extension, their isochemical melts under deep Earth conditions. Our results represent the first in-situ characterization at high pressure of glasses formed by fusion at conditions of the deep transition zone and lower mantle of the Earth.

Experimental methods

Hydrous (Mg,Fe)SiO_3 glasses were synthesized in situ at high pressure from samples of crystalline $(Mg_{0.95}Fe_{0.05})SiO_3$ enstatite from Webster, North Carolina. Enstatite powders were loaded into an Inconel gasket in a diamond-anvil cell, with characteristic sample diameters of 200 μm. A drop of distilled H_2O was added to a precompacted sample, along with a small amount of ruby (always <2% of the sample volume) on the sample surface for pressure calibration. As discussed below, this method produced samples with between 0.5 and 11 wt% H_2O. For the samples for which in-situ high pressure spectra were obtained, we used a Merrill-Bassett type diamond cell, and for samples for which we only examined spectra at ambient pressure, Mao-Bell type diamond-anvil cells were utilized. Otherwise, synthesis procedures were identical for the 19 samples examined in this study, with Type I diamonds used in all experiments. The compressed samples were melted using a continuous wave Nd:YAG laser operating in the TEM_{00} mode at 1.06 μm. Pressures were measured following melting using the ruby fluorescence method. Melting was observed visually by the onset of convective motion in the sample, with melted stripes being formed as the laser was moved across the sample. Using the spectroradiometric technique of Heinz and Jeanloz (1987) and the average to peak temperature correction of Williams et al. (1991), we estimated the melting temperature of a subset of our samples to be 1700 ± 300 K. We estimated that the quench times of our samples are faster than $\sim 10^{-5}$ s, on the basis of the thermal diffusivity of diamond and our sample thicknesses. Such rapid quench rates result in a glass transition at a higher temperature than glasses quenched at rates of only several hundred degrees per second. Some samples were decompressed immediately after synthesis, whereas others were analyzed in situ at high pressures. Spectra of quenched glasses remained unchanged after five months of storage, implying that no intergranular H_2O was present in the samples. Also, deuterated (Mg,Fe)SiO_3 glasses were synthesized to confirm the identification of bands in the H-O-H bending region and OH stretching region of the spectrum. Identical synthesis procedures were used in generating these glasses, with the substitution of 99.8% pure D_2O for H_2O.

We obtained infrared measurements during decompression of four of our high-pressure samples. Infrared spectra were obtained using a Bruker IFS-66V FTIR spectrometer, equipped with a layered InSb/MCT detector cooled by liquid N_2. After removal of base lines produced by either scattering or crystal-field absorptions of Fe^{2+}, the spectra were normalized by a frequency-dependent linear absorption coefficient (Paterson, 1982), using the integrated absorption coefficient of Stolper (1982a) for OH groups at a fixed frequency, for a hydrous glass of basaltic composition. Areas of each individual band of the OH-stretching peak, as well as the entire OH stretch region (2100–3700 cm^{-1}), were determined by integrating under the peaks, and the ratio of the concentrations of the different species producing these bands were calculated from the absorption-coefficient normalized peak areas. Using the Beer-Lambert Law, we estimated the total concentration of H_2O in our samples on the basis of these areas. For quenched glasses, thicknesses were measured using scanning electron microscopy, and we assumed a glass density of 3 g/cm^3. Table 1 shows the

TABLE 1. Weight percent H_2O in quenched samples

Synthesis *P* (GPa)	Total wt% H_2O
5.8(0.3)	1.5(0.4)
7.7(2.5)	2.2(0.6)
16.4(4.5)	0.5(0.1)*
19.5(0.3)	2.5(0.7)
21.3(3.4)	5.5(1.5)*
22.2(0.3)	3.6(1.0)
23.6(0.3)	5.2(1.4)
25.5(0.3)	11.0(3.0)
27.5(0.3)	3.9(1.0)
30.0(1.2)	10.0(2.7)
35.6(1.6)	1.0(0.3)*
37.1(0.1)	9.0(2.4)
38.7(1.9)	3.4(0.9)*
41.2(0.3)	8.0(2.2)

Note: five samples had interference fringes of sufficiently high amplitude that absolute calculations of H_2O concentrations were not reliable.
* Experiments examined in situ at high pressure.

results of the H_2O-content calculations for quenched glasses. H_2O contents range from 0.5 to 11 wt% and are below expected H_2O solubilities at the synthesis pressures of these glasses (Silver and Stolper, 1985). As the fixed absorption coefficient we used was for a basalt with 0.17 wt% H_2O, probably dissolved almost entirely as OH groups, we expect that the values in Table 1 are minimum estimates of our H_2O contents. This is because of the differing absorption coefficients of OH groups relative to OH groups bound in molecular H_2O (Newman et al., 1986).

Below ~2400 cm^{-1}, the high-pressure spectra were dominated by two-phonon and impurity absorption of the diamonds, and we were unable to observe the H-O-H bend of molecular H_2O (1450–1800 cm^{-1}) at high pressures; these bands were observed in the zero-pressure spectra of all glasses. Finally, we estimated the refractive indices of four of these glasses in the wavelength range between 2 and 5 μm, using the fringe method (Grimsditch et al., 1986) and assuming negligible dispersion over this wavelength range.

RESULTS AND DISCUSSION

Spectra of quenched glasses

Infrared spectra of six samples quenched from high pressure are shown in Figure 1. All spectra have a broad absorption band due to the primary OH stretch vibration of both molecular H_2O and OH groups (Bartholomew et al., 1980; Stolper, 1982a): the centroid of this band varies between 3400 and 2900 cm^{-1}. This band is both broad and asymmetric, with a tail to lower energies indicating that a broad distribution of H bond lengths, and thus a range of H bond strengths, exists in the glasses (Nakamoto et al., 1955; Novak, 1974; Stolper, 1982a). In several glasses (particularly those synthesized at 41 and 30 GPa), the OH absorption was sufficiently strong that the samples had very low transmission between 2900 and 3600 cm^{-1}, producing a high-frequency choppiness in this region (Fig. 1). Samples with lower H_2O contents in this same pressure regime (such as the sample synthesized at

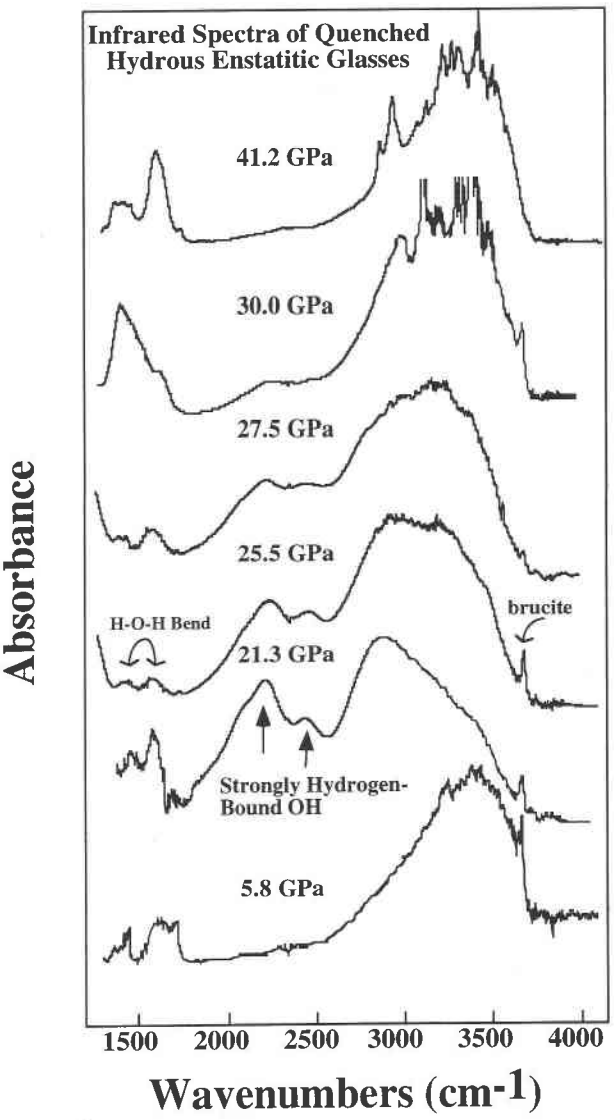

Fig. 1. Representative infrared spectra of hydrous enstatite glasses quenched from 5 to 41 GPa. The highest pressure glass has some hydrocarbon contamination, as manifested by the two peaks near 2900 cm^{-1}. Noisiness of spectra of glasses synthesized at 41 and 30 GPa results from high H_2O content of these glasses (Table 1).

38.7 GPa, whose spectrum is shown below) do not have this choppiness in the primary OH stretch region of the spectrum. We obtained an infrared spectrum of H_2O in order to confirm that there was no undissolved H_2O contributing to the spectra. This spectrum differed in both peak positions and relative amplitudes (e.g., Stevenson, 1968) from our samples, indicating that no undissolved H_2O contributed to our spectra.

In the glasses synthesized at intermediate pressures (Fig. 1), two relatively discrete peaks near 2250 and 2450 cm^{-1} occur on the low-energy side of the primary OH stretching peak. Similar bands in other silicate glasses have been assigned to strongly H-bound OH groups associated with

$^{[4]}$Si and with nonbridging O atoms (Scholze, 1959a, 1959b; Franz and Kelen, 1967; Ernsberger, 1977; Wolters and Verweij, 1981; McMillan and Remmele, 1986; Williams, 1990; Uchino et al., 1991). Scholze (1966) and Franz and Kelen (1967) assigned them to strongly H-bound SiOH groups positioned between nonbridging O atoms, whereas McMillan and Remmele (1986) attributed them to intratetrahedral H bonding: these two assignments are not necessarily exclusive. Notably, these bands cannot be due to a crystal-field transition of Fe^{2+} such as occurs in orthopyroxene at 2350 cm^{-1}, both because this transition has too broad a peak width and because its amplitude is expected to be a factor of 10^2–10^3 lower than the peaks we observe in this region of the spectrum (Goldman and Rossman, 1977).

Other interpretations of features between 2200 and 2800 cm^{-1} in hydrated alkali silicate glasses include those of Uchino et al. (1991) and Wolters and Verweij (1981), who attributed bands at 2800 and 2400 cm^{-1} in sodium silicate glasses to H bonding of molecular H_2O positioned between dipoles formed by nonbridging O and cations. Wolters and Verweij (1981) argued that the area under the bands at 2800 and 2400 cm^{-1} should occur in a constant ratio of 3:1. However, our peaks are both at different frequencies, and clearly do not show this 3:1 peak area relationship, implying that the peaks we observe are of a different origin. Uchino et al. (1991) correlate an H-O-H bending vibration at 1760 cm^{-1} and the OH vibrations at 2350 and 2800 cm^{-1} with a structurally distinct and strongly H-bound H_2O molecule. However, an inverse correlation exists between the amplitude of our peaks at 2250 and 2450 cm^{-1} and the H-O-H bend we observed at 1710 cm^{-1} (Fig. 1), thus demonstrating that these peaks are not produced by the same molecular species within our glasses. The presence of two distinct, strongly H-bound OH bands in our glasses suggests the presence of two distinct sets of Q species or two sets of O-O pairs, between which OH and H bonds can exist (i.e., two NBOs vs. one NBO and one BO: McMillan and Remmele, 1986). This is plausible on the basis of Q speciation studies, which predict that a range of Q species from Q^0 to Q^3 should be present in our quenched glasses because of the combined effects of pressure and H_2O content (Yin et al., 1983; Xue et al., 1989, 1991; Mysen, 1990; Dickinson et al., 1990).

A spectrum of a partially deuterated sample synthesized at ~32 GPa confirms that all the peaks observed above 2000 cm^{-1} are produced by OH stretching vibrations. An OD stretch band appears at ~2100 cm^{-1}, along with two features at 1870 and 1620 cm^{-1}, on the low-frequency side of the OD band. The ratio of the frequencies of these strongly H-bound peaks in hydrated samples (2450 and 2250 cm^{-1}) relative to their frequencies in the deuterated samples is 1.31 and 1.39, respectively, in approximate accord with the square root of the ratio of the reduced masses of O-H and O-D of 1.34.

Also present in the quenched spectra are peaks at 3690, 1710, 1595, and 1440 cm^{-1} (Fig. 1). The first of these is due to a small quantity of brucite (Ryskin, 1974; Kruger et al., 1989). Such brucite is an ubiquitous, but minor, product in all our syntheses. On the basis of its peak area, we estimate that it is always less than ~2% of the abundance of hydrous glass. Because brucite is present in even our lowest pressure samples (Fig. 1), it is probably produced in a cooler region of the samples, in proximity to the highly thermally conductive diamond anvils. Any crystalline SiO_2 generated by a brucite-producing reaction is unlikely to produce a signature in our OH spectra, as the solubility of H_2O in stishovite is very small (~45 ± 29 H per 10^6 Si atoms: Pawley et al., 1993). The three peaks between 1400 and 1750 cm^{-1} arise from the H-O-H bend of molecular H_2O (Scholze, 1966; Ryskin, 1974; Ernsberger, 1977; Nakamoto, 1986; Uchino et al., 1991). In some of the spectra (such as the two highest pressure spectra in Fig. 1), bands appear at 2925 and 2855 cm^{-1}, which we attribute to CH_2 stretch modes produced by minor hydrocarbon contamination of the samples (e.g., Wong and Mantsch, 1985).

The centroid frequency of the primary OH stretching peak in the ambient pressure samples is plotted as a function of synthesis pressure in Figure 2. At synthesis pressures up to 19.5 GPa, the frequency of the primary OH stretch peak shifts to lower energy with increasing pressure, reaching a minimum of ~2900 cm^{-1} near 20 GPa. This trend reverses with increasing synthesis pressure above 25 GPa. At 41.2 GPa, the frequency of this peak is 3410 cm^{-1}, nearly identical in frequency (within error) to that of the glass quenched from 5.8 GPa. Using systematics between H bond distance and OH stretching frequency, we infer that the OH···O bond distance represented by the primary OH stretching peak of the glass synthesized at 19.5 GPa is ~2.68 Å, 0.17 Å shorter than the O-H···O distance of the 5.8 GPa glass (2.85 Å) (Nakamoto et al., 1955). Thus, glasses quenched from near 20 GPa appear to contain shorter O-O distances and denser bonding configurations than the glasses quenched from either lower or higher pressures.

The amplitudes of the features at 2450 and 2250 cm^{-1} are strongly dependent on synthesis pressure. These bands have low amplitudes in the samples synthesized at 11.7 and 30 GPa and are much stronger in samples quenched from near 20 GPa, with a maximum amplitude in the glass synthesized at 21.3 GPa (Fig. 1). Between 30 and 37 GPa, these features decrease steadily in amplitude until they become unresolvable. This trend is quantified in Figure 3, which shows the ratio of the concentration of OH represented by these low-frequency peaks to OH producing the primary OH stretch peak as a function of synthesis pressure. Approximately one-fourth of the OH units in glasses quenched from near 20 GPa are present in sites with close O-O distances. Notably, the ratio of the amplitudes of these peaks appears to be independent of the total H_2O content of the glasses (Table 1).

The frequencies of these features as a function of synthesis pressure are relatively invariant (Fig. 4), with the ~2450 cm^{-1} peak shifting by only 2 cm^{-1}/GPa of syn-

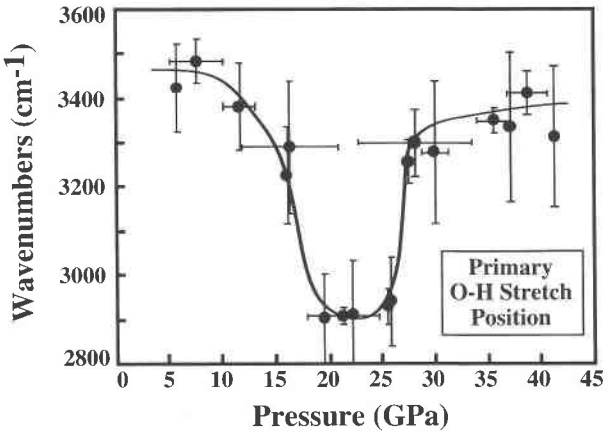

Fig. 2. OH stretch frequency of the primary OH stretching peak, as a function of synthesis pressure. The line is intended to guide the eye.

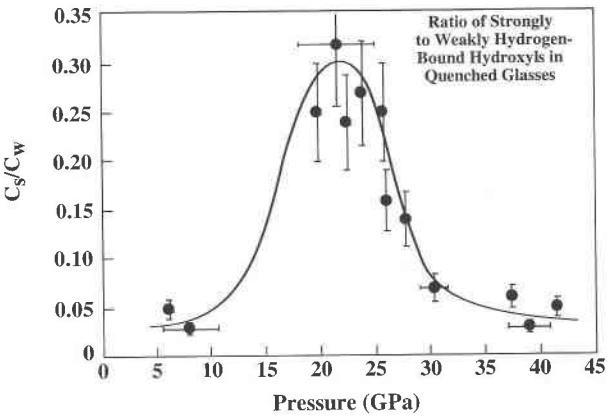

Fig. 3. Ratio of the concentration of strongly H-bound OH groups, C_s (~2500- and 2250-cm^{-1} peaks), to weakly H-bound OH groups, C_w (the primary OH stretch at between 2900 and 3400 cm^{-1}), as a function of synthesis pressure. The line is intended to guide the eye. Concentrations were obtained by dividing spectral amplitudes by a linear frequency-dependent integrated absorption coefficient (Paterson, 1982).

thesis pressure and the 2250 cm^{-1} peak showing no shift in frequency. The 2-cm^{-1}/GPa shift is particularly small relative to changes induced by synthesis pressure in the peak maximum of the primary OH stretch peak (~36 cm^{-1}/GPa of synthesis pressure: Fig. 2). The O-H···O bond lengths corresponding to the frequencies of these peaks are 2.55 and ~2.60 Å, respectively (Nakamoto et al., 1955), in contrast to the low-pressure O-H···O average bond distance of 2.85–2.90 Å. These shorter bond distances are close to the O-O bond distances in SiO_4 tetrahedra in enstatite at ambient pressure (Sasaki et al., 1982). Therefore, it is possible that these peaks are produced by intratetrahedrally H-bound OH groups, in accord with the interpretation of McMillan and Remmele (1986) about the origin of similar peaks in hydrated sodium silicate glasses. The invariance is consistent with a structural environment that remains relatively unchanged by different synthesis pressures, such as that which exists within Si tetrahedra.

Our observation that glasses quenched from between ~20 and 30 GPa have the lowest O-H stretching frequencies (Fig. 2) and the largest number of strongly H-bound OH groups (Fig. 3) is consistent with portions of the densely packed tetrahedral structure of these glasses (particularly close O-O distances) being quenchable from these pressures. However, our glasses quenched from pressures above 30 GPa have an apparent low-density configuration surrounding the OH units, with OH vibrational spectra that are essentially indistinguishable from those of glasses formed at pressures below 8 GPa.

The pressure range from which the high-density O-H···O configurations are quenched (Figs. 2 and 3), ~20–30 GPa, and above which they are not quenched, is that at which a gradual coordination change of Si from fourfold to sixfold has been documented to occur in silica, sodium silicate, diopside, and anorthite glasses (Meade et al., 1992; Wolf et al., 1990; Williams and Jeanloz, 1988). Spectroscopic and X-ray diffraction studies of glasses compressed at 300 K (Williams and Jeanloz, 1988; Wolf et al., 1990; Meade et al., 1992; Williams et al., 1993) and the phase equilibria of the crystalline phases of $MgSiO_3$ provide strong evidence for a $^{[4]}$Si to $^{[6]}$Si coordination change in this pressure regime. It is near 16 GPa that majorite, with one quarter of its Si in octahedral coordination, becomes a stable high-pressure phase in the $MgSiO_3$ system (Ohtani et al., 1986; Ito and Takahashi, 1987). Furthermore, a combination of $^{[5]}$Si and $^{[6]}$Si atoms has been documented to be present in $Na_2Si_4O_9$ glass quenched from 12 GPa at a maximum level of only 15%, with 6.3% $^{[6]}$Si. At this pressure, the stable liquidus phase of this composition has at least 25% of $^{[6]}$Si (see Fig. 3 of Xue et al., 1991). In $K_2Si_4O_9$, for which the wadeite structure is the stable crystalline polymorph (25% of Si in octahedral coordination), only 1.5% of Si in glasses quenched from 6 GPa is octahedrally coordinated (Xue et al., 1991). These results are consistent with spectroscopic and X-ray diffraction studies that have documented that $^{[6]}$Si in glasses is largely unquenchable (Williams and Jeanloz, 1988; Williams, 1990; Wolf et al., 1990; Meade et al., 1992; Williams et al., 1993). Additionally, both spectroscopic results and shock-wave experiments indicate that we should expect any coordination change of Si in liquids to occur over a broad pressure interval, with an increasing proportion of Si octahedra with increasing pressure, once the coordination change has commenced (Farber and Williams, 1992; Rigden et al., 1988). Hence, the behavior of our glasses is entirely consistent with $^{[4]}$Si undergoing a gradual and largely reversible transformation from fourfold to sixfold coordination, and we base the interpretation of our data on this framework.

The trends in Figures 2 and 3 thus indicate that glasses quenched from near 20–25 GPa represent the densest

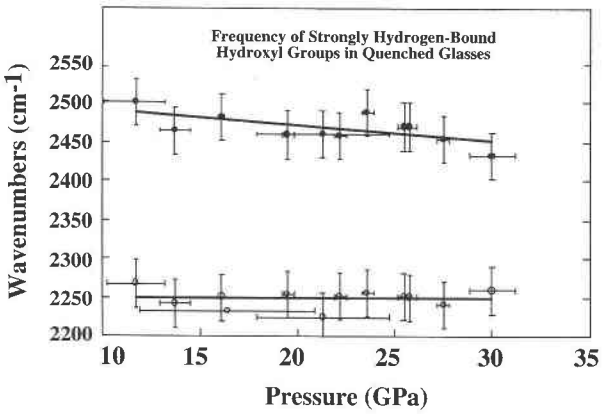

Fig. 4. Frequency of the strongly bound OH groups in pressure-quenched glasses as a function of synthesis pressure. Lines represent linear least-squares fits.

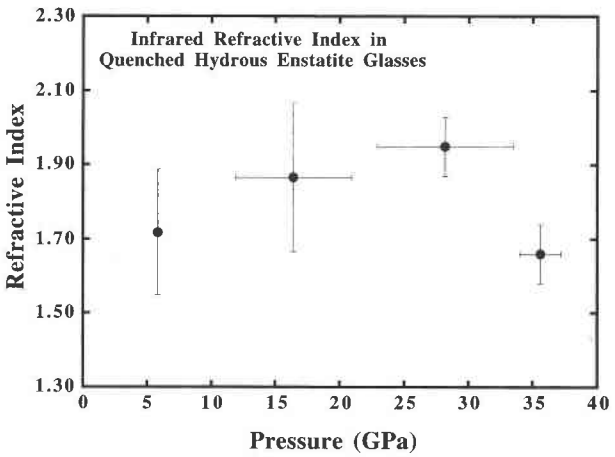

Fig. 5. Refractive indices for four glasses determined using the fringe method of Grimsditch et al. (1986). Error bars primarily reflect uncertainties in sample thicknesses.

possible glasses in which [4]Si predominates over [6]Si. It is near 25 GPa that the trade-off between densification involving tetrahedra and the associated strongly H-bound OH groups and densification by formation of Si octahedra is expected to shift in favor of [6]Si formation, resulting in a gradual decrease in the amplitude of peaks associated with tetrahedra, such that, by ~37 GPa, there are no more strongly H-bound peaks, and probably no Si tetrahedra. Hence, intratetrahedral H bonding provides a natural explanation of the frequencies and pressure range of occurrence and the invariance in frequency with respect to synthesis pressure of the strongly H-bound OH groups. Further, as we inferred from the similarity of the primary OH stretch frequency in glasses quenched from above 30 GPa to those produced at pressures below 10 GPa (Fig. 2), the rearrangement of the structure of the glass upon quench from pressures above ~30 GPa could destroy much of the high-pressure dense structure formerly present in the glass, thus explaining the absence of the strongly H-bound peaks at low frequency in the very high pressure samples. Instead, glasses quenched from the highest pressure regime record structural features that dominate at the lowest pressures on decompression, where intratetrahedral H bonding is not operative.

The measurement of four refractive indices of these glasses (Fig. 5) provides an independent check on their physical properties. In these calculations, we used the standard relationship for the interference fringes (e.g., Grimsditch et al., 1986)

$$2nd \cos \phi = K\lambda$$

where n is the refractive index, d is the sample thickness, ϕ is the angle that the light makes with the cell axis, K is the interference order (chosen arbitrarily to be an integer sequence), and λ is wavelength. Thus, a plot of $2d/\lambda$ vs. K yields a slope equal to $1/n$. The characteristic fringing we used in these calculations appears in the spectrum of a glass decompressed to 1.9 GPa from 35.6 GPa, which is shown later. As with the infrared spectral properties, the derived refractive indices are similar in the glasses quenched from below 20 GPa and above 30 GPa, demonstrating that the optical properties and thus the densities of these two sets of glasses are similar. Although the error bars are large, the data clearly indicate that glasses formed between 20 and 30 GPa are more dense than those formed at lower and higher pressures, in complete accord with our spectral observations.

Figure 6 shows spectra in the region between 1200 and 2000 cm^{-1} for quenched glasses. We attribute the peaks at 1420–1455, 1600, and 1710 cm^{-1} to the H-O-H bend of molecular H_2O and observe a dramatic increase in the amount of molecular H_2O in the glasses quenched from between 30 and 41 GPa. Although the 37 and 41 GPa samples have relatively large H_2O contents, the 25.5 GPa sample has the highest H_2O content of any in this study (Table 1). Therefore, the size of these bending peaks in the highest pressure samples is not due to the presence of larger amounts of H_2O relative to lower pressure samples. The amplitude of the 1600-cm^{-1} peak decreases slightly in the samples synthesized between 19 and 28 GPa relative to samples synthesized at lower pressures but increases dramatically in the samples synthesized from 35 GPa and above. Thus, an inverse correlation exists between the intensity of the H-O-H bend of molecular H_2O and the intensities of the peaks representing strongly H-bound OH groups, in accord with previous observations (Gennick and Harmon, 1975; Wolters and Verweij, 1981).

The frequency of the H-O-H bend moves to higher energy with increased strength of H bonding (Stevenson, 1968), and the 1710-cm^{-1} band thus represents the most strongly H-bound H_2O in our spectra. Additionally, previous results on crystalline hydroxide hydrates have indicated that the absorptivity of the H-O-H bend is decreased by H bonding (Gennick and Harmon, 1975). Accordingly, we are unable to ascertain from our quench

spectra whether the absolute amount of molecular H_2O in our glasses is less in the pressure interval between ~20 and 25 GPa, or whether the strong H bonding present in these glasses simply decreases the absorptivity of the H-O-H bending vibration, thereby decreasing the amplitude of these peaks. However, since the frequency of these peaks does not shift in glasses quenched from the strongly H-bound regime between 20 and 30 GPa, we believe that a decrease in the amount of molecular H_2O between these pressures provides the most straightforward explanation for the amplitude of the bending vibrations.

High-pressure spectra

In order to examine the degree to which our quenched spectra reflect the structure of glasses at high pressures, we conducted a sequence of experiments to examine the structure of glasses at their synthesis pressures and during decompression. Figure 7 shows three sets of spectra obtained on decompression from ~39, 36, and 21 GPa. The broad primary OH stretch absorption band is present in all spectra, along with the weak brucite absorption near ~3690 cm^{-1}. Also, a feature with varying amplitude appears at a frequency near ~2500 cm^{-1} on the shoulder of the primary OH stretch peak in all samples. Within the 38.7-GPa sample, this feature is present only at the highest pressures, whereas in the 35.6-GPa sample there is amplitude in this spectral region to pressures of 1.9 GPa (Fig. 7B). In the sample synthesized at 21 GPa, this feature is associated with the quenched strongly H-bound peaks of Figures 1, 3, 4, and 6.

In all three samples, the frequency of the OH stretch peak maximum gradually increases with decreasing pressure, starting near 2700 cm^{-1} or lower at 38.7 GPa, near ~2900 cm^{-1} or lower at 35.6 GPa, and near 2900 cm^{-1} at 21.3 GPa (Fig. 7). The exact maximum of this peak is difficult to determine in the highest pressure samples because of both overlap with the neighboring peak at lower energy and our diamond-produced lower spectral cutoff. The primary OH stretch frequency of 2700 cm^{-1} observed in the 38.7-GPa sample corresponds to an O-H $\cdots$O distance of 2.64 Å (Nakamoto et al., 1955). Half this distance, 1.32 Å, is slightly shorter than the anionic radius of O^{2-} in twofold coordination at ambient pressure (1.35 Å: Shannon and Prewitt, 1969). Moreover, it is similar to the radius of O in both stishovite and $MgSiO_3$ perovskite (Sinclair and Ringwood, 1978; Horiuchi et al., 1987). Thus, it appears that the volume of O-H groups is close to that of the volume of O^{2-} ions at pressures of 39 GPa and above. For comparison, half of the O-O bond distance in this glass after quenching is 1.43 Å.

In the sample synthesized at 21.3 GPa, the frequencies of the primary O-H stretch at 6.4 GPa and at ambient pressure are 3139 and 2908 cm^{-1}, respectively, indicating that complex changes in the relative amplitudes of different components of this band take place on quench at low pressures (Fig. 7C). In this sample, a weak shoulder is present on the low-energy side of the OH stretch peak maximum near ~2810 cm^{-1}. This shoulder is weakly visible at 14.2 GPa and becomes more apparent as the maximum of the principal OH stretch peak moves to higher energy upon decompression. It is possible that the species associated with the zero-pressure peak maximum is the same as that which produces this shoulder in the high-pressure spectra, with a frequency at ambient pressure ~100 cm^{-1} higher than at 21 GPa. We observe similarly complex behavior of different components of the primary OH stretch for a sample synthesized at 28 GPa. We attribute this shift in ambient pressure position of the primary O-H stretch peak for samples synthesized between ~16 and 30 GPa (Fig. 2) to a changing range of OH-group environments with decreasing pressure, with those OH molecules with longer O-O distances and thus higher energy vibrations spreading out over a broad range of frequencies upon quenching.

The feature that occurs near 2500 cm^{-1} in the high-pressure spectra only quenches in the glass synthesized at

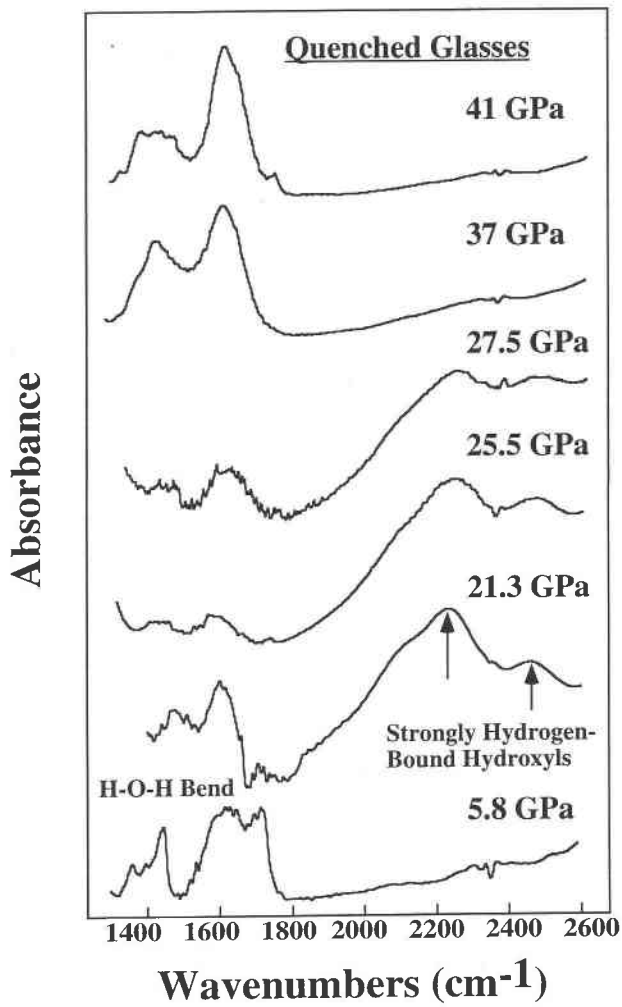

Fig. 6. Ambient-pressure infrared spectra of glasses synthesized between 5 and 41 GPa in the region of the strongly H-bound OH stretch and H-O-H bending vibrations (1350–2600 cm^{-1}).

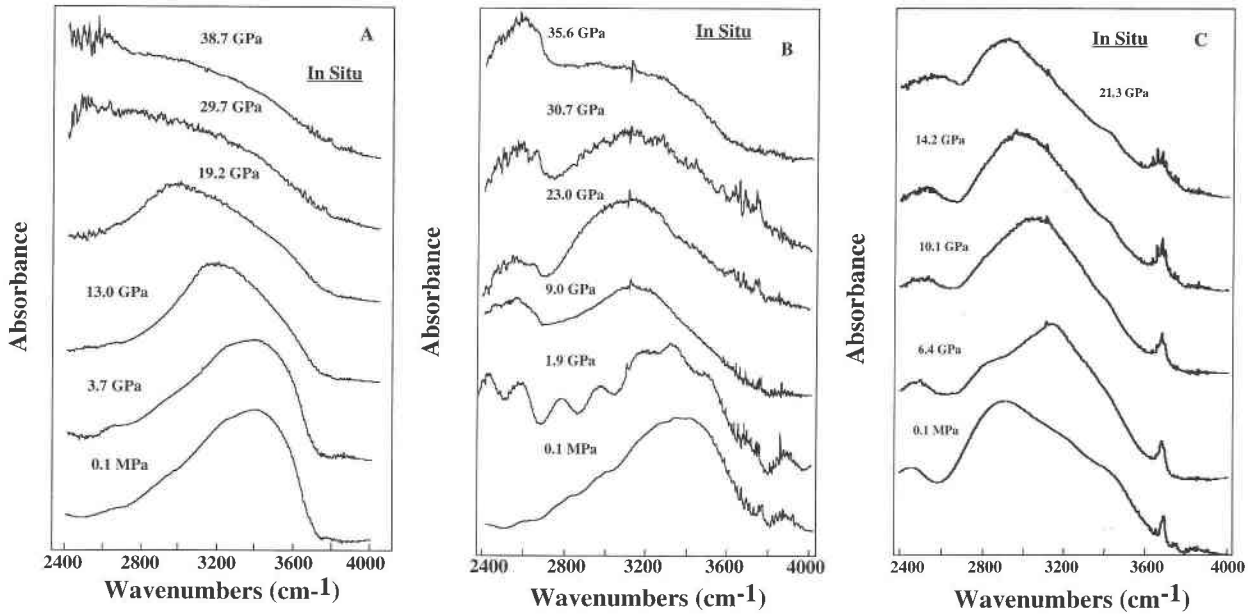

Fig. 7. Infrared spectra of hydrous enstatite glass on decompression from synthesis pressures of 38.7 (**A**), 35.6 (**B**), and 21.3 GPa (**C**). All three sets of spectra show the spectra of the quenched glasses at the bottom. Minor interference from atmospheric H_2O vapor is present in **B** and **C** at frequencies near 3700 cm^{-1}. In **B**, the 1.9-GPa spectrum shows the heavy fringing characteristic of samples used for refractive index measurements. This fringing was eliminated by damaging the surface of the decompressed sample. Note that in contrast to the zero-pressure spectrum (**B**), the strongly H-bound OH peak at ~2500 cm^{-1} is present in the 1.9-GPa spectrum but is obscured by fringing.

21.3 GPa. In the 38.7 GPa it disappears below 29 GPa or shifts to the portion of the spectrum we did not obtain, whereas in the 35.6-GPa glass it persists down to 1.9 GPa (Fig. 7B). We note that in minerals with all or most of their Si in octahedral coordination, OH stretch vibrations occur at notably low frequencies, as in stishovite, with an OH stretch vibration at 3111 cm^{-1} (Pawley et al., 1993), and phase D, with its most intense vibration at 3270 cm^{-1} (Williams, 1992). Our association of the peaks at ~2250 and 2450 cm^{-1} in the quenched spectra with dense tetrahedral environments and their absence in the samples quenched from above 30 GPa suggest that no Si tetrahedra existed in the highest pressure glasses. We therefore associate the unquenchable low frequencies of the OH stretch in the spectra of the samples synthesized at 38.7 and 35.6 GPa with environments involving higher coordinations of Si. That strongly H-bound OH species persist to pressures below 10 GPa in the glasses synthesized at above 30 GPa indicates a large amount of hysteresis exists in the conversion of Si octahedra to tetrahedra (e.g., Stolper and Ahrens, 1987; Williams et al., 1993). This supports the idea of a decompressional mechanism for the highest pressure glasses (>35 GPa) whereby hysteresis of the $^{[6]}Si$ to $^{[4]}Si$ conversion results in adjustment of the structural features of the glass to $^{[4]}Si$ at relatively low pressures (below ~5–10 GPa), where other pressure-induced structural changes, such as intratetrahedral H bonding, would not be operative.

In Figure 8A, the pressure shifts of the primary OH stretch peak for two sets of decompression spectra are shown. The zero-pressure frequencies are excluded from the linear fits to the mode shifts because of the unusual quench behavior of these glasses. As shown in Figure 8A, the absolute location of the primary OH stretch peak upon decompression shows a broad variation in different samples, as a result of both the difficulty in locating this peak and shifts in band shape on decompression. However, the markedly increased frequency of the primary OH stretching peak with decreasing pressure demonstrates that as these glasses decompress, major decreases in the strength of H bonding and increases in O-O distance occur.

The feature at ~2500 cm^{-1}, in contrast to the primary O-H stretch, shows a weak decrease in frequency with decreasing pressure (Fig. 8B). A positive pressure shift is unusual for H-bonded species (e.g., Williams, 1992) and could indicate that on decompression the O-O distances associated with this species actually decrease; more likely, the amount of cation-H repulsion (with the cations being H or Mg) could be decreasing on decompression. In the 35.6-GPa sample, this peak shows only a slight dependence on pressure (Fig. 8B), but in the sample synthesized at 21.3 GPa, the shift is larger (~5 cm^{-1}/GPa: Fig. 8A, 8B). Thus, rapid overall changes in the OH structural environment apparently occur on decompression from 21.3 GPa, whereas only modest changes occur on decompression from 35.6 GPa (until this band disappears at low pressures). This nonquenchability of the 2500-cm^{-1} feature in the two highest pressure samples, when coupled

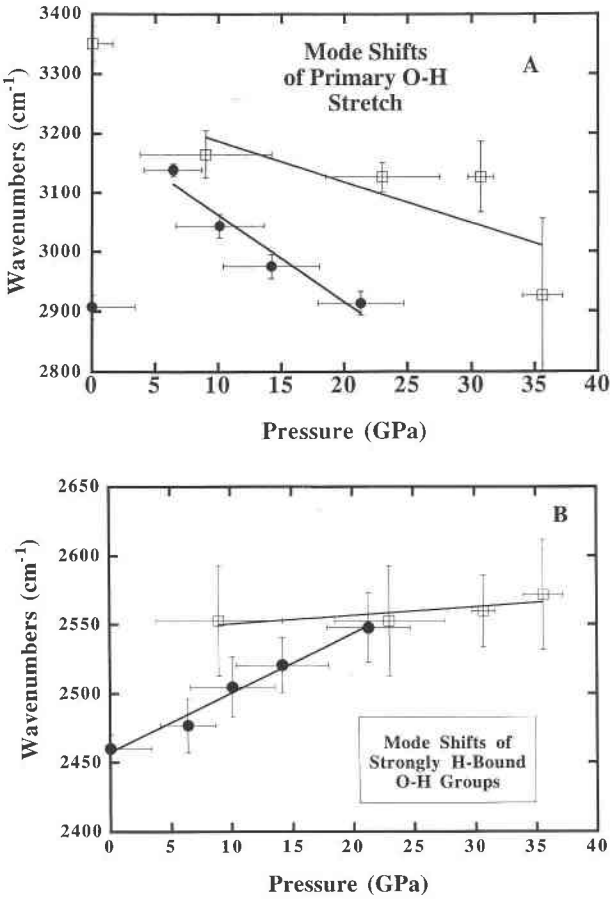

Fig. 8. Mode shifts of OH stretch vibrations in glasses synthesized at 35.6 and 21.3 GPa. Solid circles represent the 21.3-GPa glass, open squares, the 35.6-GPa glass. (**A**) Frequency of the primary OH stretch peak vs. pressure. Frequencies of the ambient-pressure spectra are not included in the linear fits of the mode shifts because of the complex rearrangement of the band envelope on quench in these glasses. (**B**) Pressure dependence of the frequency of the strongly H-bound OH groups. The ambient pressure frequency of the 35.6-GPa glass is not included because of its nonquenchability to zero pressure.

with the difference in pressure dependences, documents that the bands in this spectral region have a different origin in the higher pressure samples than in the lower pressure samples.

The frequency of the unquenchable peak at 2500 cm^{-1} in samples synthesized above 30 GPa, with which we have associated Si in octahedral coordination, is consistent with what would be expected for intraoctahedral H bonding. Indeed, ~2500 cm^{-1} corresponds to an OH···O bond distance of ~2.60 Å (Nakamoto et al., 1955), close to the O-O bond distances in $MgSiO_3$ perovskite (~2.53 Å: Horiuchi et al., 1987). Because O-O bond distances calculated from the systematics of Nakamoto et al. (1955) are for linear OH···O groups, our inferred bond length estimates represent maximum estimates, as any bending of the OH···O group would shorten the actual O-O bond length. The larger positive pressure shift of the H-bound OH groups associated with intratetrahedral OH groups could be correlated with changes in tetrahedral distortion known to accompany high pressure glass compression (Hemley et al., 1986; Williams and Jeanloz, 1988; Williams et al., 1993).

TABLE 2. Peak areas and species concentrations on decompression in a sample synthesized at 35.6 GPa

P (GPa)	Area (×10^3)	C_s	C_s/C_w
35.6(1.6)	1.307	0.10(0.03)	0.25(0.11)
30.7(1.0)	2.024	0.08(0.02)	0.12(0.04)
23.0(4.5)	2.125	0.06(0.02)	0.08(0.03)
9.0(5.2)	2.028	0.05(0.01)	0.07(0.03)
0.1 MPa	2.940	0.05(0.01)	0.05(0.02)

Note: area = area under entire OH peak, includes both C_s and C_w; determined after normalization by integrated absorption coefficient. C_s = concentration of strongly H-bound OH groups, as determined by integration under the ~2500-cm^{-1} peak. C_s/C_w = ratio of the concentration of strongly H-bound OH to weakly bound OH, determined by the difference between total weight percent H_2O and C_s. Numbers in parentheses represent errors limits based on uncertainties in density, thickness, integrated absorbance, ϵ^* (at 3550 cm^{-1}), and $d\epsilon^*/d\nu$.

To constrain the number of strongly H-bound OH molecules and the pressure dependence of the extinction coefficient, we calculated the relative concentrations of both strongly H-bound OH groups (~2500 cm^{-1}) and the OH groups under the primary OH stretch band from the peak areas at each pressure in the spectra of the sample synthesized at 35.6 GPa (Table 2). Not surprisingly, the relative concentration of strongly H-bound OH molecules decreases on decompression. However, the overall integrated intensity under the OH bands increases by about a factor of two on decompression. This change in band intensity plausibly reflects a decrease with pressure of the extinction coefficient of the OH species, possibly produced by a pressure-induced change in the charge distribution around the O ion (and thus an altered dipole moment of the OH stretch). Such a pressure dependence of the extinction coefficient could be crucial in determining H_2O content and H_2O speciation of glasses at high pressures. Because of the low total H_2O content of this sample (~1 wt%), most of the H_2O in this glass is dissolved as OH groups. Therefore, the peak areas of these spectra are primarily sensitive to the extinction coefficient of OH groups, and not to a mixture of OH and H_2O groups (e.g., Newman et al., 1986).

In Figure 9, we speculate on one way in which H_2O may facilitate a coordination change in our glasses quenched from the $^{[6]}$Si regime. This largely geometric model includes features that plausibly are present in our glasses and structural characteristics on which we can draw constraints from the known bond distances of high-pressure silicate phases. In Figure 9a, the addition of H_2O to a corner-sharing $^{[6]}$Si network results in breakage of bridging O atoms between octahedra, and the formation of intraoctahedral H bonding, with OH···O bond distances of ~2.55–2.60 Å. Each octahedron contains two nonbridging O atoms (NBOs) and four bridging O atoms

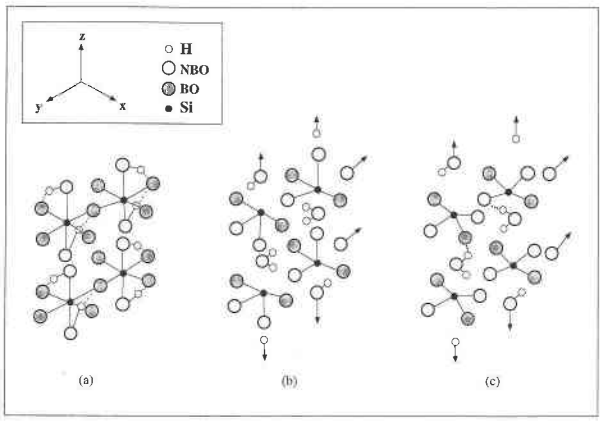

Fig. 9. Schematic of possible mechanism by which H_2O depolymerizes Si octahedra and facilitates the transformation from $^{[6]}$Si to $^{[4]}$Si on decompression. Bridging O atoms are all within the **x**-**y** plane, as defined by the axes in the figure, forming sheets of corner-sharing octahedra. (**a**) Fully polymerized Si octahedral network depolymerized by addition of one molecule of H_2O per octahedron, generating intraoctahedral O-O bond distances of ~255 pm; after addition of H_2O, there are 4 O atoms per Si, resulting in two nonbridging O atoms (NBO) per octahedron and four bridging O atoms (BO) per octahedron. All four BOs lie within the **x**-**y** plane, generating sheets of corner-sharing octahedra. (**b**) Si octahedra undergoing a coordination change, with the loss of one BO and two NBOs per octahedron. This is achieved when two bonds are broken: one to a OH-bound O and one to a H-bound O. H_2O molecules are formed. (**c**) The stabilization of the network after undergoing the coordination change, with weak H bonding forming at the lowest pressures on decompression. In **b** and **c** the chains of tetrahedra run parallel to the **x** axis.

(BOs). On decompression, the glass reverts to $^{[4]}$Si, with the loss of one NBO and two BOs per octahedron by breakage of two bonds per octahedron (Fig. 9b). One Si-O bond involving a OH-bound NBO, and one Si-O bond involving a H-bound BO, are broken. The bonds associated with OH or H-bound O atoms are expected to be weaker than Si-O bonds that do not involve H. When an O atom and its associated H atoms are lost from the polyhedron, they could form molecular H_2O by bonding to a H from the adjacent polyhedron (Fig. 9b). In Figure 9c, chains of point-shared tetrahedra form (parallel to the **x** axis). The protons in the H_2O molecules form weak H bonds to nearby O atoms at the lowest pressures on decompression. This simple scenario for the reversion of $^{[6]}$Si to $^{[4]}$Si would generate the abundance of molecular H_2O we observe in our glasses quenched from above 35 GPa, the lack of strongly H-bound OH units in these glasses, and the notable decrease in H bonding of the glass observed on decompression.

Implications and conclusions

Under pressure, the frequency of the primary OH stretch peak in our glasses decreases markedly, indicating that stronger H bonding is an important densification mechanism of OH in hydrous glasses throughout the pressure range of this study. Yet, between ~19 and 28 GPa, the observed mode of densification of these glasses gradually changes. The low frequency (near 2900 cm^{-1}) of the primary OH stretching peak upon quench from this pressure range, its higher frequency (~3400 cm^{-1}) on quench from above 30 GPa, and the unquenchability of the strongly H-bound OH vibrations from above 30 GPa suggest that the dominant mode of densification above 30 GPa is not preserved on quench (Figs. 1 and 2). The lack of similarity of the spectra of glasses above 30 GPa to their quenched products is consistent with most of the features in the glasses at high pressure being associated with Si in sixfold coordination. Also, the resemblance of these glasses at zero pressure to those synthesized at the lowest pressures of this study is consistent with a relatively low-pressure reversion of $^{[6]}$Si to $^{[4]}$Si. At the low pressures at which this reversion plausibly occurs, low-pressure densification mechanisms are reflected in the spectra of the quenched glasses. Therefore, the most plausible interpretation of our results is that $^{[4]}$Si and $^{[6]}$Si coexist up to ~37 GPa, but with an increasing proportion of $^{[6]}$Si (and possibly $^{[5]}$Si) with increasing pressure starting at ~20 GPa. Quenching our hydrous glasses from pressures at which sixfold coordination plausibly predominates, above 30 GPa, results in the destruction of many high-pressure structural characteristics as the glass structure undergoes reconstructive changes upon quench. Our data provide the first evidence for such major reconstructive changes in glasses formed at high pressure and examined in situ at their pressure of synthesis. Additionally, we associate both the ability to quench the low-frequency OH stretching vibration peak (near 2900 cm^{-1}) and the presence of peaks on the low-energy side of the primary OH stretch peak with irreversible densification of glasses within a dominantly tetrahedrally coordinated regime.

The structure of a hydrous (Mg,Fe)SiO_3 glass under high pressure has implications for element partitioning and melt buoyancy in the deep Earth. A melt similar to this composition could plausibly be generated at high temperatures in a hydrous assemblage in the deep Earth, thereby modulating the occurrence of deep-mantle hydrous phases. Sixfold-coordinated melts may be negatively or neutrally buoyant in the deep Earth and, if they are hydrous, such melts could transport or retain volatiles in the deep Earth. Moreover, H_2O in melts at high pressures clearly adopts structurally dense configurations, and we therefore suggest that modeling hydrous melts exclusively as mixed oxides (including H_2O) is not consistent with our spectroscopic data and structural interpretations. Indeed, it is likely from our inferred O-O bond distances that H_2O dissolves in silicate melts at high pressures in a manner that is consistent with simply introducing one O atom per H_2O molecule into the silicate network; that is, the volume occupied by hydroxide units in an octahedral network is probably similar to that occupied simply by O^{2-} anions. Such a dissolution mechanism, in which the volume of H_2O is entirely modulated

by the volume of O^{2-} in compressed melts, could produce very dense hydrous melts such as have been inferred to exist in hydrous assemblages under shock-loading conditions (Tyburczy et al., 1991).

Acknowledgments

Work supported by the NSF [to E. Knittle (C.C.) and Q.W.] and the W.M. Keck Foundation. Contribution no. 245 of the Institute of Tectonics (Mineral Physics Lab) at UCSC. We thank D. Farber, H. Keppler, and an anonymous reviewer for helpful comments and suggestions.

References cited

Acocella, J., Tomozawa, M., and Watson, E.B. (1984) The nature of dissolved water in sodium silicate glasses and its effect on various properties. Journal of Non-Crystalline Solids, 65, 355–372.

Agee, C.B., and Walker, D. (1988) Static compression and olivine flotation in ultrabasic silicate liquid. Journal of Geophysical Research, 93, 3437–3449.

——— (1993) Olivine flotation in mantle melt. Earth and Planetary Science Letters, 114, 315–324.

Bartholomew, R.F., Butler, B.L., Hoover, H.L., and Wu, C.K. (1980) Infrared spectra of a water-containing glass. Journal of the American Ceramic Society, 63, 481–485.

Dickinson, J.E., Jr., Scarfe, C.M., and McMillan, P. (1990) Physical properties and structure of $K_2Si_4O_9$ melt quenched from pressures up to 2.4 GPa. Journal of Geophysical Research, 95, 15675–15681.

Dziewonski, A.M., and Anderson, D.L. (1981) Preliminary reference Earth model. Physics of the Earth and Planetary Interiors, 25, 297–356.

Eckert, H., Yesinowski, J.P., Silver, L.A., and Stolper, E.M. (1988) Water in silicate glasses: Quantitation and structural studies by ^1H solid echo and MAS-NMR methods. Journal of Physical Chemistry, 92, 2055–2064.

Ernsberger, F.M. (1977) Molecular water in glass. Journal of the American Ceramic Society, 60, 91–92.

Farber, D.L., and Williams, Q. (1992) Pressure-induced coordination changes in alkali-germanate melts: An in situ spectroscopic investigation. Science, 256, 1427–1430.

Franz, H., and Kelen, T. (1967) Erkenntnisse über die Struktur von Alkalisilicatgläsern und schmelzen aus dem Einbau der OH-Gruppen. Glastechnische Berichte, 40, 141–148.

Gennick, I., and Harmon, K.M. (1975) Hydrogen bonding: VI. Structural and infrared spectral analysis of lithium hydroxide monohydrate and cesium and rubidium hydroxide hydrates. Inorganic Chemistry, 14, 2214–2219.

Goldman, D.S., and Rossman, G.R. (1977) The spectra of iron in orthopyroxene revisited: The splitting of the ground state. American Mineralogist, 62, 151–157.

Grimsditch, M., Letoullec, R., Polian, A., and Gauthier, M. (1986) Refractive index determination in diamond anvil cells: Results for argon. Journal of Applied Physics, 60, 3479–3481.

Heinz, D.L., and Jeanloz, R. (1987) Temperature measurements in the laser-heated diamond cell. In M. Manghnani and Y. Syono, Eds., High pressure research in mineral physics, p. 113–127. American Geophysical Union, Washington, DC.

Hemley, R.J., Mao, H.K., Bell, P.M., and Mysen, B.O. (1986) Raman spectroscopy of SiO_2 glass at high pressure. Physical Review Letters, 57, 747–750.

Hetherington, G., and Jack, K.H. (1962) Water in vitreous silica: I. Influence of 'water' content on the properties of vitreous silica. Physics and Chemistry of Glasses, 3, 129–133.

Horiuchi, H., Ito, E., and Weidner, D.J. (1987) Perovskite-type $MgSiO_3$: Single-crystal X-ray diffraction study. American Mineralogist, 72, 357–360.

Ito, E., and Takahashi, E. (1987) Melting of peridotite at uppermost lower-mantle conditions. Nature, 328, 514–517.

Kruger, M.B., Williams, Q., and Jeanloz, R. (1989) Vibrational spectra of $Mg(OH)_2$ and $Ca(OH)_2$ under pressure. Journal of Chemical Physics, 91, 5910–5915.

Kubicki, J.D., Hemley, R.J., Hofmeister, A.M. (1992) Raman and infrared study of pressure-induced structural changes in $MgSiO_3$, $CaMgSi_2O_6$, and $CaSiO_3$ glasses. American Mineralogist, 77, 258–269.

Kümmerlen, J., Merwin, L.H., Sebald, A., and Keppler, H. (1992) Structural role of H_2O in sodium silicate glasses: Results from ^{29}Si and ^1H NMR spectroscopy. Journal of Physical Chemistry, 96, 6405–6410.

McMillan, P., and Piriou, B. (1983) Raman spectroscopic studies of silicate and related glass structure—A review. Bulletin de Minéralogie, 106, 57–75.

McMillan, P.F., and Remmele, R.L., Jr. (1986) Hydroxyl sites in SiO_2 glass: A note on infrared and Raman spectra. American Mineralogist, 71, 772–778.

Meade, C., Hemley, R.J., and Mao, H.K. (1992) High-pressure X-ray diffraction of SiO_2 glass. Physical Review Letters, 69, 1387–1390.

Miller, G.H., Stolper, E.M., and Ahrens, T.J. (1991) The equation of state of a molten komatiite: I. Shock wave compression to 36 GPa. Journal of Geophysical Research, 96, 11831–11848.

Mysen, B.O. (1990) Effect of pressure, temperature, and bulk composition on the structure and species distribution in depolymerized alkali aluminosilicate melts and quenched melts. Journal of Geophysical Research, 95, 15733–15744.

Nakamoto, K. (1986) Infrared and Raman spectra of inorganic and coordination compounds (4th edition), 484 p. Wiley-Interscience, New York.

Nakamoto, K., Margoshes, M., and Rundle, R.E. (1955) Stretching frequencies as a function of distances in hydrogen bonds. Journal of the American Chemical Society, 77, 6480–6486.

Newman, S., Stolper, E.M., and Epstein, S. (1986) Measurement of water in rhyolitic glasses: Calibration of an infrared spectroscopic technique. American Mineralogist, 71, 1527–1541.

Novak, A. (1974) Hydrogen bonding in solids: Correlation of spectroscopic and crystallographic data. Structure and Bonding, 18, 177–216.

Ohtani, E., Kato, T., and Sawamoto, H. (1986) Melting of a model chondritic mantle to 20 GPa. Nature, 322, 352–353.

Paterson, M.S. (1982) The determination of hydroxyl by infrared absorption in quartz, silicate glasses and similar materials. Bulletin de Minéralogie, 105, 20–29.

Pawley, A.R., McMillan, P.F., and Holloway, J.R. (1993) Hydrogen in stishovite, with implications for mantle water content. Science, 261, 1024–1026.

Revenaugh, J., and Sipkin, S.A. (1994) Seismic evidence of silicate melt atop the 410-km mantle discontinuity. Nature, 369, 474–476.

Rigden, S.M., Ahrens, T.J., and Stolper, E.M. (1984) Densities of liquid silicates at high pressures. Science, 226, 1071–1074.

——— (1988) Shock compression of a molten silicate: Results for a model basaltic composition. Journal of Geophysical Research, 93, 367–382.

Ryskin, Ya.I. (1974) The vibrations of protons in minerals. In V.C. Farmer, Ed. The infrared spectra of minerals, p. 137–181. Mineralogical Society, London.

Sasaki, S., Takeuchi, Y., Fujino, K., and Akimoto, S. (1982) Electron-density distributions of three orthopyroxenes $Mg_2Si_2O_6$, $Co_2Si_2O_6$, and $Fe_2Si_2O_6$. Zeitschrift für Kristallographie, 158, 279–297.

Scholze, H. (1959a) Der Einbau des Wassers in Gläsern, I. Glastechnische Berichte, 32, 81–88.

——— (1959b) Der Einbau des Wassers in Gläsern, II. Glastechnische Berichte, 32, 142–152.

——— (1966) Gases and water in glass, II. The Glass Industry, 47, 622–628.

Shannon, R.D., and Prewitt, C.T. (1969) Effective ionic radii in oxides and fluorides. Acta Crystallographica, B25, 925–936.

Shelby, J.E., and McVay, G.L. (1976) Influence of water on the viscosity and thermal expansion of sodium trisilicate glasses. Journal of Non-Crystalline Solids, 20, 439–449.

Silver, L., and Stolper, E. (1985) A thermodynamic model for hydrous silicate melts. Journal of Geology, 93, 161–176.

Sinclair, W., and Ringwood, A.E. (1978) Single crystal analysis of the structure of stishovite. Nature, 272, 714–715.

Stevenson, D.P. (1968) Molecular species in liquid water. In A. Rich and N. Davidson, Eds., Structural chemistry and molecular biology, p. 491–497. Freeman and Company, San Francisco, California.

Stolper, E.M. (1982a) Water in silicate glasses: An infrared spectroscopic study. Contributions to Mineralogy and Petrology, 81, 1–17.

———(1982b) The speciation of water in silicate melts. Geochimica et Cosmochimica Acta, 46, 2609–2620.

Stolper, E.M., and Ahrens, T.J. (1987) On the nature of pressure-induced coordination changes in silicate melts and glasses. Geophysical Research Letters, 14, 1231–1233.

Susman, S., Volin, K.J., Liebermann, R.C., Gwanmesia, G.D., and Wang, Y. (1990) Structural changes in irreversibly densified fused silica: Implications for the chemical resistance of high level nuclear waste glasses. Physics and Chemistry of Glasses, 31, 144–150.

Tomozawa, M. (1985) Water in glass. Journal of Non-Crystalline Solids, 73, 197–204.

Tyburczy, J.A., Duffy, T.S., Ahrens, T.J., and Lange, M.A. (1991) Shock wave equation of state of serpentine to 150 GPa: Implications for the occurrence of water in the Earth's lower mantle. Journal of Geophysical Research, 96, 18011–18027.

Uchino, T., Sakka, T., and Iwasaki, M. (1991) Interpretation of hydrated states of sodium silicate glasses by infrared and Raman analysis. Journal of the American Ceramic Society, 74, 306–313.

Watson, E.B. (1981) Diffusion in magmas at depth in the Earth: The effects of pressure and dissolved H_2O. Earth and Planetary Science Letters, 52, 291–301.

White, B.S., and Montana, A. (1990) The effect of H_2O and CO_2 on the viscosity of sanidine liquid at high pressures. Journal of Geophysical Research, 95, 15683–15693.

Williams, Q. (1990) Molten $(Mg_{0.88}Fe_{0.12})_2SiO_4$ at lower mantle conditions: Melting products and structure of quenched glasses. Geophysical Research Letters, 17, 635–638.

———(1992) A vibrational spectroscopic study of hydrogen in high pressure mineral assemblages. In Y. Syono and M.H. Manghnani, Eds., High pressure research: Application to Earth and planetary sciences, p. 289–296. American Geophysical Union, Washington, DC.

Williams, Q., and Jeanloz, R. (1988) Spectroscopic evidence for pressure-induced coordination changes in silicate glasses and melts. Science, 239, 902–905.

Williams, Q., Knittle, E., and Jeanloz, R. (1991) The high-pressure melting curve of iron: A technical discussion. Journal of Geophysical Research, 96, 2171–2184.

Williams, Q., Hemley, R.J., Kruger, M.B., and Jeanloz, R. (1993) High-pressure infrared spectra of α-quartz, coesite, stishovite and silica glass. Journal of Geophysical Research, 98, 22157–22170.

Wolf, G.H., Durben, D.J., and McMillan, P.F. (1990) High-pressure Raman spectroscopic study of sodium tetrasilicate ($Na_2Si_4O_9$) glass. Journal of Chemical Physics, 93, 2280–2288.

Wolters, D.R., and Verweij, H. (1981) The incorporation of water in silicate glasses. Physics and Chemistry of Glasses, 22, 55–61.

Wong, P.T.T., and Mantsch, H.H. (1985) Pressure effects on the infrared spectrum of 1,2-dipalmitoyl phosphatidycholine bilayers in water. Journal of Chemical Physics, 83, 3268–3274.

Wu, C. (1980) Nature of incorporated water in hydrated silicate glasses. Journal of the American Ceramic Society, 63, 453–457.

Xue, X., Stebbins, J.F., Kanzaki, M., and Tronnes, R.G. (1989) Silicon coordination and speciation changes in a silicate liquid at high pressures. Science, 245, 962–964.

Xue, X., Stebbins, J.F., Kanzaki, M., McMillan, P.F., and Poe, B. (1991) Pressure-induced silicon coordination and tetrahedral structural changes in alkali oxide-silica melts up to 12 GPa: NMR, Raman, and infrared spectroscopy. American Mineralogist, 76, 8–26.

Yin, C.D., Okuno, M., Morikawa, H., and Marumo, F. (1983) Structure analysis of $MgSiO_3$ glass. Journal of Non-Crystalline Solids, 55, 131–141.

Manuscript received May 19, 1994
Manuscript accepted November 28, 1994